JOURNAL OF GEOPHYSICAL RESEARCH, VOL. 115, A04303, doi:10.1029/2009JA014829, 2010

Temporal modulations of the longitudinal structure in F_2 peak height in the equatorial ionosphere as observed by COSMIC

Guiping Liu,[1] Thomas J. Immel,[1] Scott L. England,[1] Karanam K. Kumar,[2] and Geetha Ramkumar[2]

Received 24 August 2009; revised 14 October 2009; accepted 16 November 2009; published 1 April 2010.

[1] This study investigates the temporal variability of longitudinal structure in F_2 layer peak height (h_mF_2) in the equatorial ionosphere. For this study, electron density profiles retrieved from the radio occultation measurements by the Constellation Observing System for Meteorology, Ionosphere, and Climate (COSMIC) are fitted with a two-layer Chapman function to determine h_mF_2. The h_mF_2 values in the magnetic equatorial region display a four-peaked longitudinal structure that has been identified in other ionospheric observations. The four-peaked structure is likely the signature of the forcing by the eastward propagating nonmigrating diurnal tide with zonal wave number 3 (DE3). Further analysis for the period of prominent four-peaked structure over August-September 2008 finds that this structure exhibits a 5 day periodicity. Coincidentally, the all-sky interferometric meteor radar's wind measurements at Thumba (8.5°N, 77°E) in India for the mesosphere and lower thermosphere indicate strong 5 day planetary waves within that time period. The observed temporal periodicity of the four-peaked longitudinal structure in h_mF_2 could thus be attributed to the interaction of DE3 with a 5 day planetary wave.

Citation: Liu, G., T. J. Immel, S. L. England, K. K. Kumar, and G. Ramkumar (2010), Temporal modulations of the longitudinal structure in F_2 peak height in the equatorial ionosphere as observed by COSMIC, *J. Geophys. Res.*, *115*, A04303, doi:10.1029/2009JA014829.

1. Introduction

[2] The plasma in the ionospheric F region (at 200–600 km altitude) is densest at latitudes 15°–20° away from the magnetic equator, giving it a two-banded longitudinally extended structure [*Namba and Maeda*, 1939; *Appleton*, 1946]. This phenomenon is often referred to as the equatorial ionospheric anomaly (EIA). The EIA is produced by the process of the so-called fountain effect, where the plasma is lifted during the day by dynamo electric fields driven by winds in the lower ionosphere (E region).

[3] The features of the EIA have been determined from a number of different measurement techniques. The EIA was first discovered from ground-based measurements and has been investigated recently by means of space-borne instruments for observing airglow emissions [e.g., *Carruthers and Page*, 1976; *Thuillier et al.*, 2002]. These observations have revealed a global-scale pattern in the emission rate of airglow that corresponds to the ionospheric plasma density.

[4] More recently, it has been found that the OI airglow emission at 135.6 nm wavelength exhibits a longitudinal variation with four peaks [*Sagawa et al.*, 2005; *Henderson et al.*, 2005]. A similar four-peaked structure has also been observed in the ionospheric total electron content using radio occultation measurements [*Lin et al.*, 2007; *Scherliess et al.*, 2008].

[5] The longitudinal four-peaked structure in the equatorial F region could be caused by the eastward propagating nonmigrating diurnal tide with zonal wave number 3 (DE3) [e.g., *Immel et al.*, 2006; *England et al.*, 2006, 2009]. Nonmigrating tides excited in the troposphere by latent heat released by condensing water vapor can propagate upward to the ionospheric E region, there approaching wind speeds of the magnitude of tens of meters per second [*Hagan and Forbes*, 2002, 2003; *Oberheide and Forbes*, 2008]. It is believed that tidal modulation of the background winds in the low-latitude and midlatitude E region can modify the dynamo electric fields that produce the EIA and thereby extend the tidal effect to the equatorial F region. Indeed, simulations from the thermosphere-ionosphere-mesosphere electrodynamics general circulation model (TIME-GCM) with the tidal forcing at the lower boundary at 30 km altitude have demonstrated that the zonal wave number 4 pattern in F region plasma density is the result of the upward and poleward plasma drifts, caused mainly by dynamo action of the DE3 diurnal tide [*Hagan et al.*, 2007].

[6] *Immel et al.* [2009] reported that the F region longitudinal four-peaked structure may undergo a periodic modu-

[1]Space Sciences Laboratory, University of California, Berkeley, California, USA.
[2]Space Physics Laboratory, Vikram Sarabhai Space Centre, Trivandrum, India.

0148-0227/10/2009JA014829

lation. They found a 6 day periodicity in the power of the wave number 4 signature in both the separation and the density of the EIA. The authors proposed that this periodicity could be due to the interaction of the diurnal tide with longer-period planetary waves. The effects of waves with periods of several days have previously been observed in the *F* region [e.g., *Chen*, 1992; *Forbes et al.*, 1996; *Pancheva et al.*, 2006, 2008; *Pedatella and Forbes*, 2009]. Numerical predictions have suggested that the stationary planetary wave 4 modulates the DE3 tide and may impact ionospheric signatures [*Hagan et al.*, 2009]. However, understanding the subsequent impact of the interaction of the planetary waves with the tides requires more observation-based investigations.

[7] This study focuses on the longitudinal variations of the ionospheric F_2 layer peak height (h_mF_2) at the magnetic equator. The purpose of the study is to search for the four-peaked structure in h_mF_2 and its periodic modulations by planetary waves, which has not been studied in any detail before. The study utilizes the ionospheric measurements of the Constellation Observing System for Meteorology, Ionosphere, and Climate (COSMIC) and the wind measurements in the mesosphere and lower thermosphere by the meteor radar at Thumba (8.5°N, 77°E) in India. The data utilized in the study are described in section 2. The retrieval of the F_2 layer peak height by COSMIC is assessed, and the COSMIC electron density profiles are used to determine h_mF_2. These are presented in section 3. The results of the study are discussed at length in section 4. The h_mF_2 values in the magnetic equatorial region have a prominent four-peaked longitudinal structure during 17 August to 16 September 2008. This is consistent with the seasonal variation of the DE3 that has larger amplitude at this time. The h_mF_2 are grouped by "every *n*th day" (as described in section 4) during this time interval of prominent four-peaked structure, and it is found that over the period, the amplitude of this structure exhibits a 5 day periodicity. The coincident wind measurements from the meteor radar at Thumba indicate strong 5 day planetary wave activity in the mesosphere and lower thermosphere. This suggests that the 5 day periodicity of the four-peaked structure in h_mF_2 could be attributed to the interaction of DE3 with this 5 day planetary wave.

2. COSMIC and Meteor Radar at Thumba, India

[8] COSMIC is a satellite constellation for measuring properties of the atmosphere and the ionosphere through the GPS radio occultation technique [*Cheng et al.*, 2006; *Schreiner et al.*, 2007]. COSMIC is a collaborative mission between Taiwan and the United States. It was launched in April 2006 into a circular low Earth orbit at about 500 km altitude. The mission has successfully operated, providing unprecedented information on ionospheric variations.

[9] Six identical microsatellites constitute the COSMIC constellation system. They were initially launched into the same orbit, and then during the following 13 months, they were gradually spread to individual orbits at a higher altitude of about 800 km. Since late 2007, the satellites have operated on their final orbits with the inclination of 72° and orbital planes separated by 24° longitude.

[10] The multiple satellites of COSMIC can make measurements throughout the day, having the ability to cover 24 h full local time for a given latitude in one single day. However, the coverage is not uniform and the sampling is irregular because of the fact that the COSMIC-GPS occultations are not preplanned. Figure 1a shows the local time coverage of the daily COSMIC measurements in 2008 in the equatorial region (geographic latitudes of 20°S–20°N). These measurements have gaps in local time on each day, but certain local times can be measured by COSMIC continuously across many days. As an example, the data for days 230–260 (17 August to 16 September 2008) cover the local time range of 15–17 h for every day. Studies in this local time range provide a measure of the effect of the daytime ionospheric electric dynamo. Studies during this part of the year provide a good opportunity to study the DE3 tide that has been found to have larger amplitude during June–September [e.g., *Forbes et al.*, 2008]. Therefore, this period of data in this local time range is selected for this study.

[11] The all-sky interferometric meteor (SKiYMET) radar at Thumba (8.5°N, 77°E) is a multichannel coherent radar [*Kumar et al.*, 2007]. This radar system operates at 35.25 MHz with a peak power of 40 kW. The radar measures the drift of meteor trails that are used to deduce the speed and the direction of the wind. As currently operated, the altitude resolution of this meteor radar is 2 km. The meteor echoes are grouped in altitude such that there will be sufficient echoes to allow a statistically significant estimate of the winds. The wind observations of the radar are at 82, 85, 88, 91, 94, and 98 km height regions. Hourly zonal and meridional winds are available.

[12] The SKiYMET radar at Thumba was operated continuously in 2008 except for a few days of interruptions. The wind measurements of the radar have enabled the study of planetary waves with periods of 2–30 days and their interactions with the diurnal tides [*Kumar et al.*, 2008]. The radar at Thumba is located at the dip equator and therefore provides an excellent complement to the equatorial COSMIC observations used in this study. In the study, the radar wind data over the same period as COSMIC (17 August to 16 September 2008) are used to identify the planetary waves in the mesosphere and lower thermosphere within that time period. Measuring the correspondence of the ionospheric structure with the planetary waves is the goal of the study, and this is discussed later in section 4.

3. COSMIC Electron Density Profiles

[13] COSMIC measures the vertical profiles of refractivity in the atmosphere and the ionosphere using radio occultations. Through this technique, vertical profiles of ionospheric electron density can be retrieved. Normally, 1500–2000 electron density profiles are provided per day, each with a vertical resolution of about 1 km. These profiles are distributed unevenly in latitude with most of them falling at midlatitudes and high latitudes. The number of the profiles in the equatorial region, within ±20° latitude, is smaller (~300 per day).

[14] To assess the data quality, the electron density profiles from COSMIC are compared with coincident incoherent

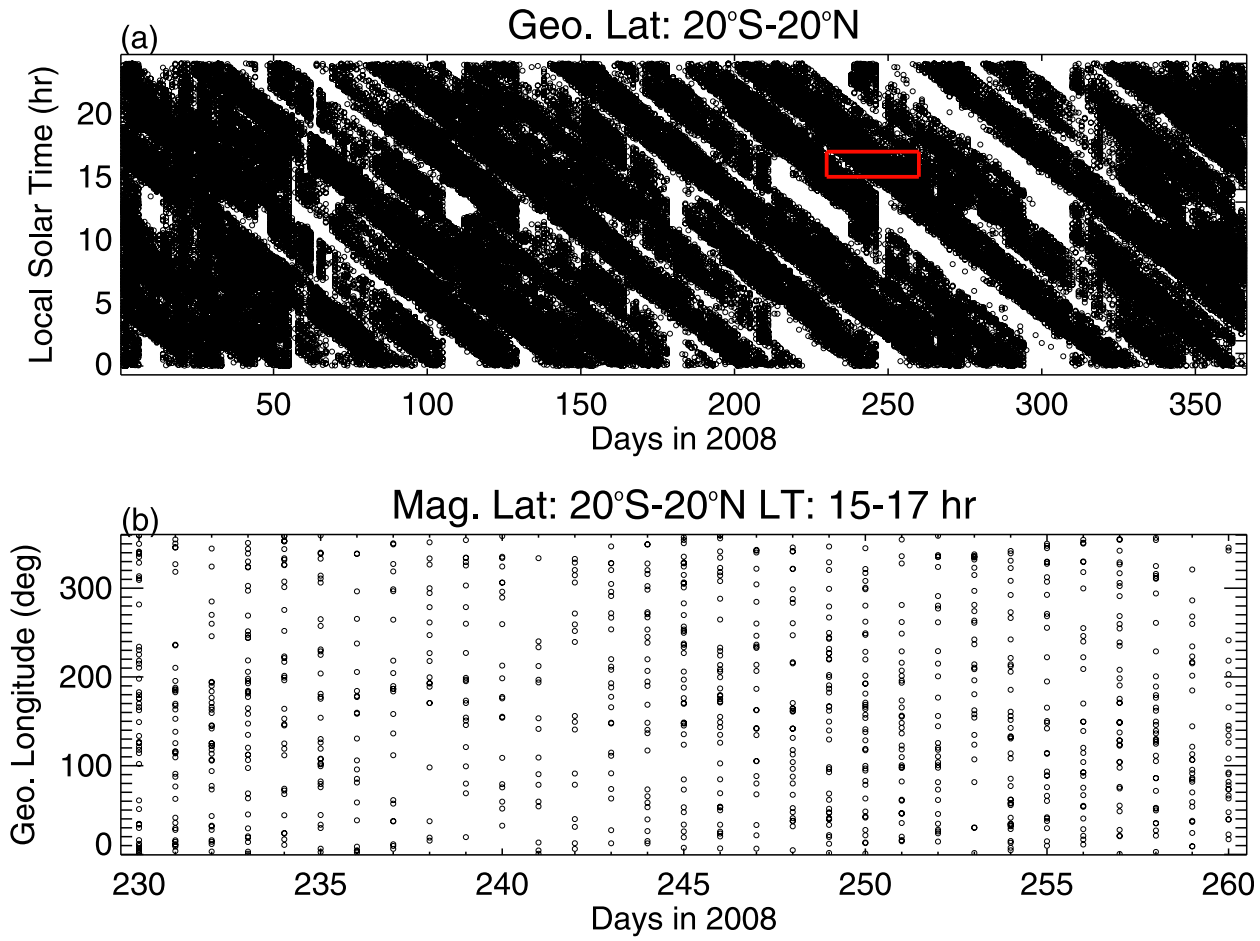

Figure 1. (a) Local time coverage of daily measurements in 2008 by COSMIC in the equatorial region between ±20° latitude. The red box marks the data for days 230–260 (17 August to 16 September 2008) and local times of 15–17 h. (b) Longitudinal coverage of the COSMIC measurements over 17 August to 16 September 2008 in the magnetic equatorial region for the local times of 15–17 h.

scatter radar (ISR) data. Figure 2 shows the comparison for Jicamarca (11.9°S, 76.0°W). The profiles within 3° latitude, 8° longitude, and 1 h time difference between COSMIC and the ISR in July 2008 are shown. For the comparison, the ISR profiles are averaged for 1 h time intervals. The horizontal bars in the profiles represent the standard deviation of the mean electron density observed during the hour. The plots show that the shape of the electron density profiles is similar for both COSMIC and the Jicamarca ISR, where both show a single F_2 layer with the density peak near 300 km altitude. The magnitudes of the F_2 layer peak density differ, but the heights of the peaks are virtually the same. Similarly, the COSMIC electron density profiles have been compared with the Millstone Hill ISR (42.6°N, 71.5°W) data (plots are not included), and their F_2 layer peak heights are also similar.

[15] The ionospheric measurements of COSMIC have been assessed for its early launch period in 2006 [*Lei et al.*, 2007; *Kelley et al.*, 2009]. Here, the general agreement with the ISR for the F_2 layer peak height is reinforced for a different time period, and the agreement holds for both the low-latitude and midlatitude sites. This suggests that the retrieval of the F_2 peak height by COSMIC is reliable.

[16] To determine h_mF_2, the COSMIC electron density profiles are fitted with a two-layer Chapman function [*Fox*, 1994; *Lei et al.*, 2007]. Profiles with large error are screened out. Only profiles having more than eight points of data in the altitude range of 150–600 km are selected and are then fitted through least squares fitting. Only profiles having a fitting error (percentage difference between the fits and the data) of less than 10% are used.

4. Longitudinal Wave Number 4 Structure and 5 Day Variation

[17] Figure 3a shows the variation of h_mF_2 in relation to geographic longitude and latitude. The h_mF_2 values determined from the COSMIC electron density profiles in the local time range of 15–17 h during 17 August to 16 September 2008 are binned for 15° longitude and 5° latitude intervals and are shown in Figure 3. The blank area indicates heights uniformly lower than 240 km, reflecting the extreme solar minimum conditions [e.g., *Heelis et al.*, 2009]. Figure 3 shows that h_mF_2 has the largest values within ±30° latitude and forms a band pattern along the magnetic equator. The h_mF_2 values are larger at the north of

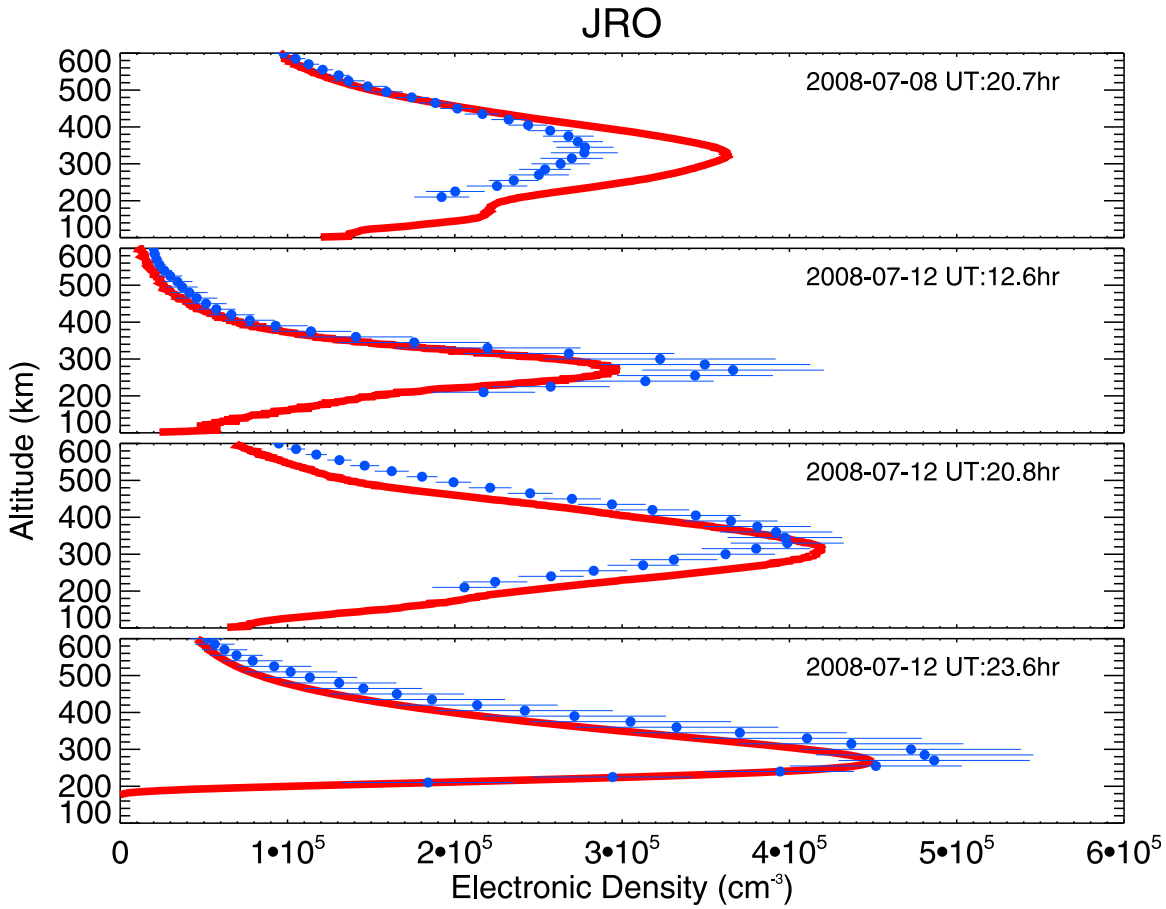

Figure 2. Electron density profiles from COSMIC (red curve) and the Jicamarca ISR (blue dots) for the same location (within 3° latitude and 8° longitude) and same time (within 1 h difference). The horizontal blue bars are the standard deviation of the ISR data within the 1 h time intervals. The times of the COSMIC measurements are given in the plots. Note that the vertical resolution of COSMIC data is about 1 km, while the Jicamara ISR is for 15 km.

the magnetic equator than at the south of the equator. This asymmetry of h_mF_2 is likely due to transequatorial F region winds [*Thuillier et al.*, 2002]. The winds during the period blow from the Northern Hemisphere to the Southern Hemisphere and push plasma along the magnetic field, raising the height of the F_2 layer at locations north of the equator while reducing h_mF_2 to the south.

[18] Figure 3a also indicates that along the magnetic equator, the h_mF_2 values change with longitude. There is an extended longitudinal range of large h_mF_2 over Pacific and South America, with additional peaks in Africa and eastern Asia. Many factors, such as the magnetic declination [*Hartman and Heelis*, 2007] and field strength [*Schunk and Nagy*, 2000], F region winds [*Thuillier et al.*, 2002], and, most important for the purposes of this study, nonmigrating tides [*England et al.*, 2009], play a role in producing this longitudinal structure. These tides are believed to be responsible for the underlying wave number 4 structure, which is evident in Figure 3b.

[19] The h_mF_2 values in the magnetic equatorial region at 15–17 h local time from 17 August to 16 September 2008 are shown in Figure 3b. This is for the same time period as in Figure 3a but is limited to magnetic latitudes within ±20°. These h_mF_2 values are binned in 15° longitude intervals and are then fitted for a sinusoidal wave with wave number 4. The four-peaked longitudinal structure is dominant. This is consistent with the signature forced by the nonmigrating DE3 tide.

[20] In order to identify the day-to-day variation, the equatorial h_mF_2 data in individual days from 17 August to 16 September 2008 at the given local time of 15–17 h are now grouped by every nth day. This grouping is needed to improve the sampling and fill data gaps in longitude on each day (see Figure 1b). For each individual day, most of the 15° longitude bins include one to three data points. Grouping the data for several days increases the number of samples in each bin by a factor of 3–5. In this study, the h_mF_2 values from 17 August to 16 September are binned into n series with each series containing the values from every nth day (e.g., for the case of n = 5, five series are created with the first series containing data from days 1, 6, 11, 16, 21, 26, the second series containing data from days 2, 7, 12, 17, 22, 27, etc.). For this period, series are created for n = 4, 5, 6, 7, and 8. For n = 4, the series contains at least 7 days of data; for n = 8, at most only 4 days of data are included in each series.

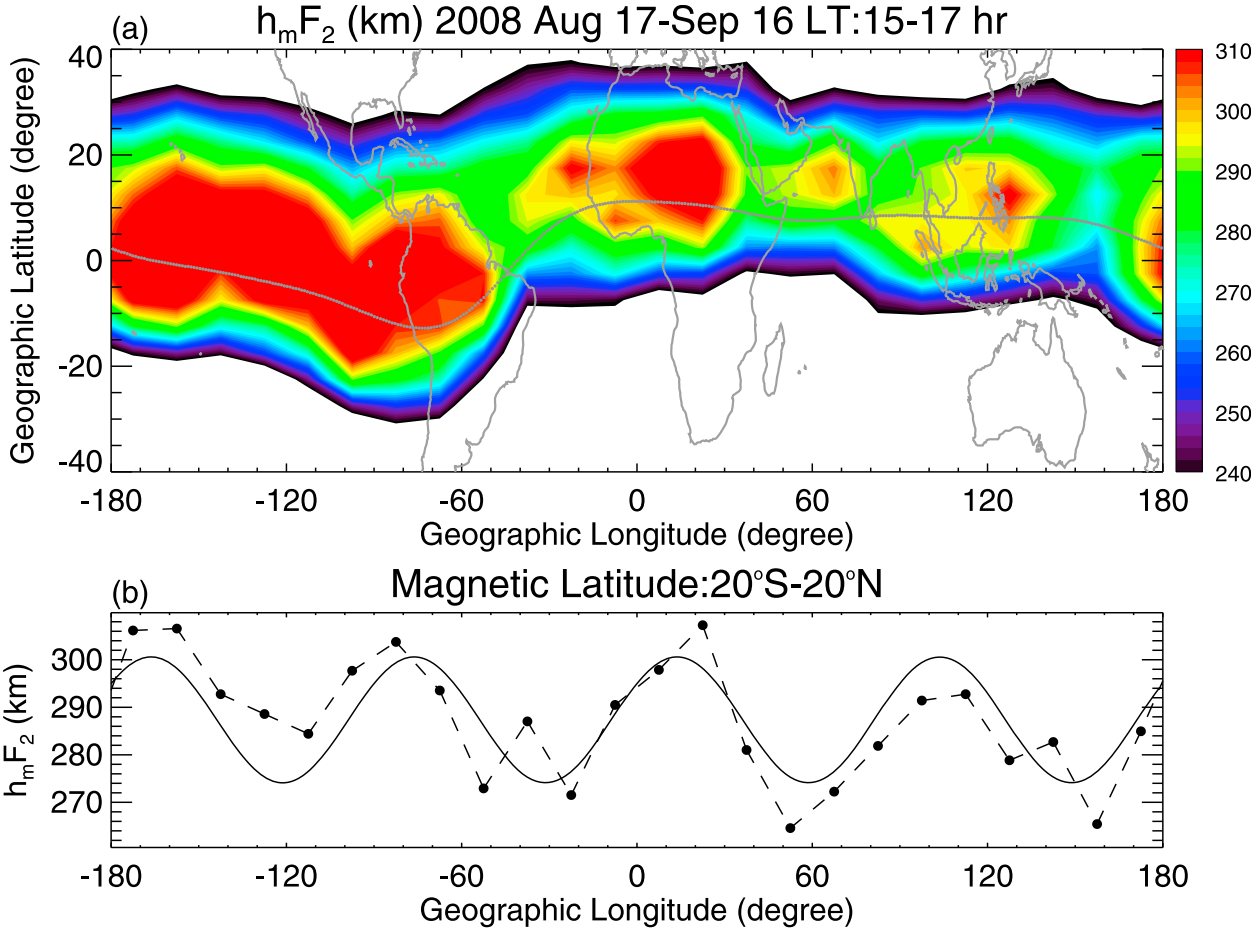

Figure 3. (a) F_2 layer peak heights (h_mF_2) from the COSMIC electron density profiles at the given local time range of 15–17 h during the period of 17 August to 16 September 2008. The black line indicates the magnetic equator. (b) h_mF_2 values in the magnetic equatorial region at 15–17 h local time during 17 August to 16 September 2008 shown by the dot-dashed line. The curve superimposed is from the wave number 4 harmonic fits.

[21] As an example, Figure 4 displays the series for $n = 5$. Each series includes a wave number 4 structure in h_mF_2, having four peaks along the magnetic equator. The same structure is seen in each series, but the amplitude of the structure varies. The four peaks are stronger in the first, the second, and the third series but are weaker in the fourth and the fifth series. This suggests a temporal variation of the four-peaked structure.

[22] To quantify the amplitude variation of the h_mF_2 four-peaked structure, the power of the wave number 4 component in each series is calculated through the fast Fourier transform (FFT). The FFT powers are given in Figures 5a–5e for $n = 4$ to $n = 8$. The curves in Figures 5a–5e are from harmonic fits for sinusoidal waves with periods of 4–8 days, respectively. The fitting errors (percentage difference between the fits and the data) are presented in Figure 5f. The plots indicate that the wave number 4 power tends to follow a 5 day variation.

[23] The 5 day periodicity in the longitudinal wave number 4 structure of h_mF_2 indicates that the apparent forcing by the DE3 diurnal tide suffers a 5 day modulation. This variation could correspond to a 5 day planetary wave. To identify which planetary waves are present in the equatorial mesosphere and lower thermosphere within the same time period, zonal wind measurements from the SKiYMET radar at Thumba are used.

[24] The radar wind measurements at Thumba during the period of 17 August to 16 September 2008 are analyzed with a wavelet transformation to retrieve temporal periodicity. The wavelet spectra for both 91 and 98 km altitudes (Figure 6) reveal strong 5 day waves in late August 2008. To characterize this 5 day planetary wave, the radar zonal wind measurements at different altitudes (82–98 km) are band pass filtered for the period of 4–6 days (centered on day 5 with a width of 2 days). This analysis method of wave properties has been described in detail by *Takahashi et al.* [2006] and *Pancheva et al.* [2008].

[25] The results shown in Figures 7a–7f indicate that the 5 day wave occurs between days 235 and 250 and lasts for about 15 days (also seen in Figure 6). For this study, the COSMIC data through the entire period of 17 August to 16 September are binned in order to identify the 5 day wave signature. This binning includes the data from days when the 5 day wave in the mesosphere and lower thermo-

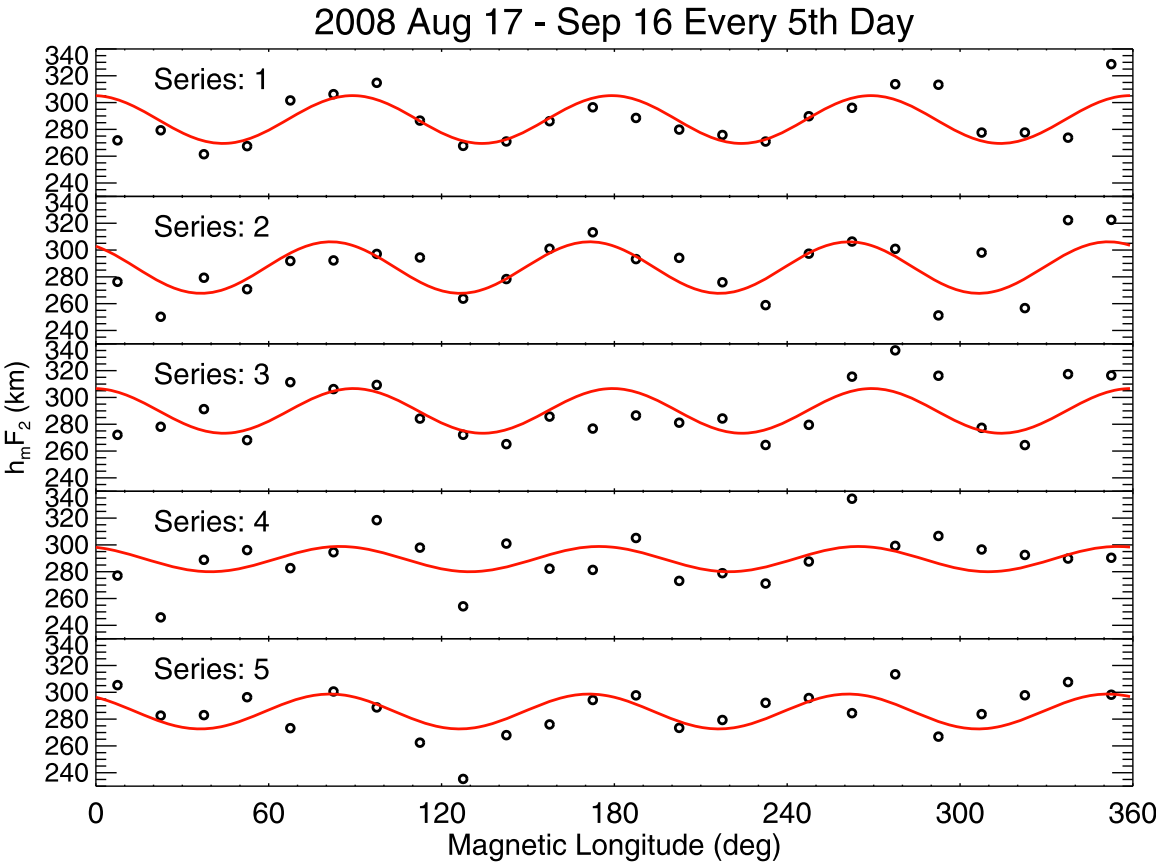

Figure 4. Longitudinal structure of h_mF_2 from every fifth day grouping as denoted by circles. The red curves are from the wave number 4 harmonic fits.

sphere is both strong and weak. The 5 day wave signature in COSMIC is likely reduced by this binning. An improved spatial and temporal sampling would likely reveal a stronger 5 day wave signature in the ionosphere.

[26] Figure 7g gives the phase of this 5 day planetary wave over a range of altitudes, indicating an upward propagating wave with a vertical wavelength of 37 ± 3 km. This wavelength is significantly larger than the 6 day fast Kelvin wave [*Hirota*, 1979]. The period of this 5 day wave does not match with that of the 3–4 day ultrafast Kelvin wave [*Forbes*, 2000]. The closest matching wave is the 5 day Rossby wave; however, it is worth noting that the 37 km vertical length of this wave does not fully agree with that previously observed [e.g., *Wu et al.*, 1994; *Pancheva et al.*, 2008]. A further investigation with the aid of another radar station at the same latitude as Thumba but separated in longitude would be needed in order to determine the type of wave seen here.

5. Discussion and Conclusions

[27] This study finds temporal modulations of the four-peaked longitudinal structure in h_mF_2 in the equatorial ionosphere by a planetary wave. Previous work by *Immel et al.* [2009] found a similar periodicity of the ionospheric wave number 4 structure but did not provide complimentary evidence of the presence of the planetary wave. This study, for the first time, identifies the planetary wave in the mesosphere and lower thermosphere that causes the periodicity in the wave number 4 structure in the ionosphere using simultaneous observations of both the neutral atmosphere and the ionosphere.

[28] The temporal periodicity of the four-peaked longitudinal structure in the ionosphere suggests an interaction of the DE3 with the planetary wave. The DE3 can be a dominant tide in the *E* region [*Forbes et al.*, 2006], and a number of planetary waves can propagate into the *E* region as well [e.g., *Laštovička*, 2006; *Mukhtarov et al.*, 2009; *Pancheva et al.*, 2009a, 2009b]. The interaction between the tide and the planetary wave could occur in the *E* region [e.g., *Fritts and Vincent*, 1987; *Teitelbaum and Vial*, 1991; *Pancheva et al.*, 2006; *Kumar et al.*, 2008] or at altitudes below in the mesosphere or lower thermosphere. Because the SKiYMET radar does not provide observations throughout this altitude range, investigating this aspect must be left to a future study.

[29] Both tides and planetary waves can modify the *E* region dynamo and thus extend their effects into the *F* region. Signatures of these drivers have been observed in previous ionospheric measurements [e.g., *Forbes et al.*, 1996; *Immel et al.*, 2006; *Pancheva et al.*, 2006, 2008; *Pedatella and Forbes*, 2009]. However, the consequence of the interaction between them has not been noticed with much attention. Space-based observations provide a global

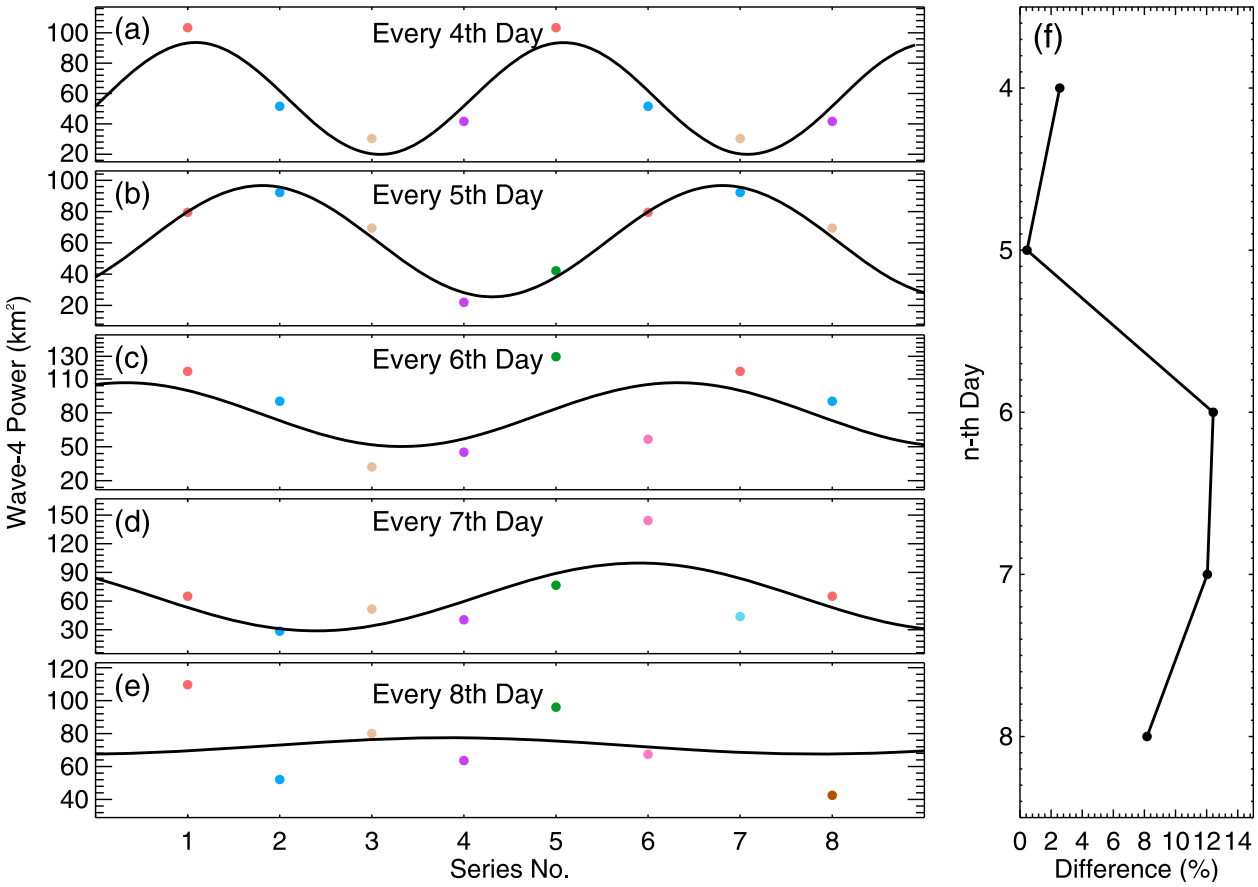

Figure 5. FFT power of wave number 4 component from (a) every 4th day grouping, (b) every fifth day grouping, (c) every sisxth day grouping, (d) every seventh day grouping, and (e) every eighth day grouping. The superimposed curves on Figures 5a–5e are from the harmonic fits with 4–8 days waves, respectively. (f) Percentage difference of the fits to the data.

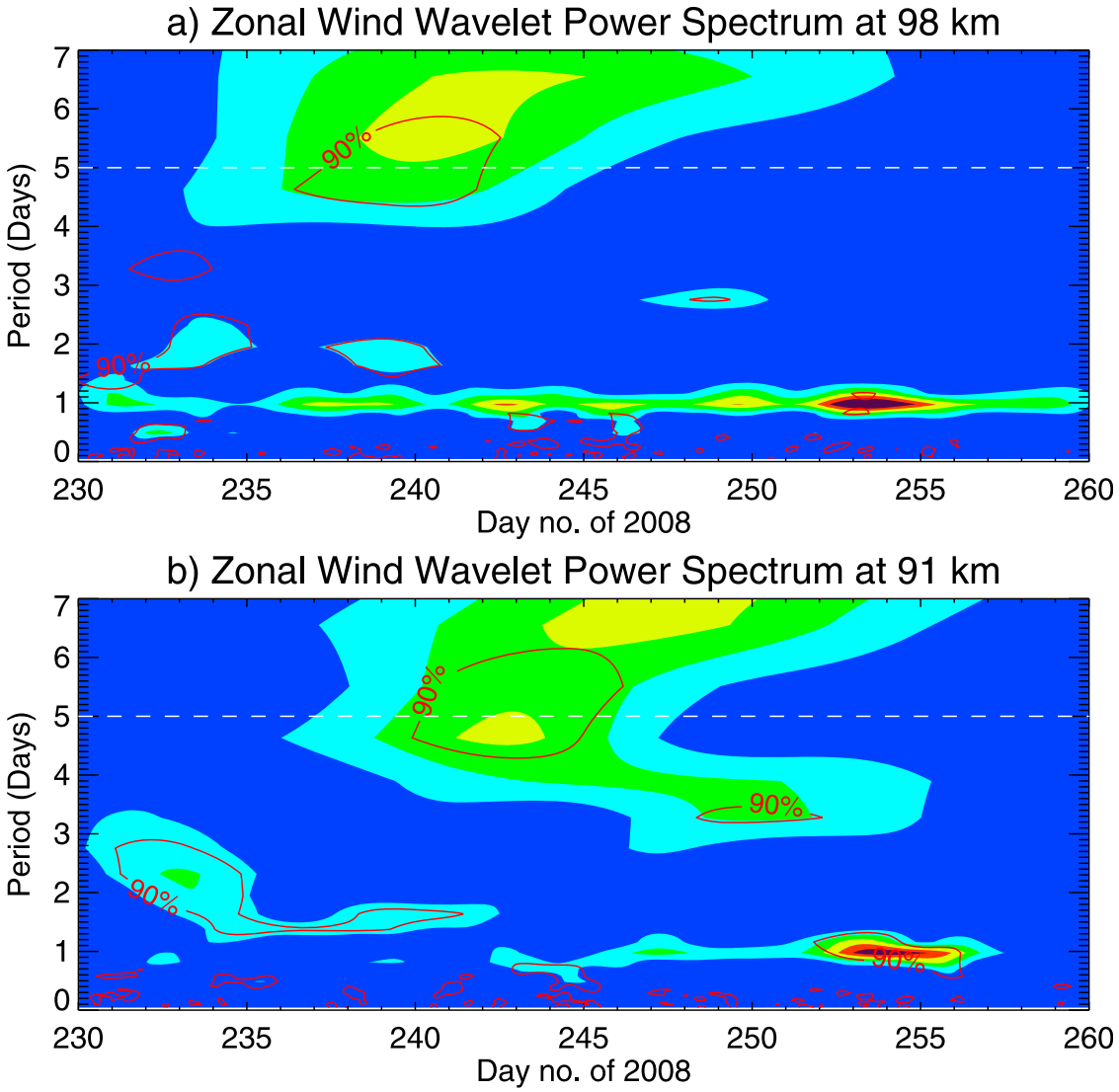

Figure 6. Wavelet power spectrum of hourly zonal winds from the SKiYMET radar at Thumba (8.5°N, 77°E) during the period of 17 August to 16 September 2008 for (a) 98 km altitude and (b) 91 km altitude. The contour levels in Figures 6a and 6b are for 10,000, 20,000, 30,000, 40,000, and 50,000 m^2 s^{-2} and 5000, 10,000, 15,000, 20,000, and 25,000 m^2 s^{-2}, respectively. The red contours denote the 90% significance levels, and the white dashed lines highlight the 5 day period. Note that the missing data are filled with the yearly means of 2008 for the wavelet transformation.

view of ionospheric variability and can reveal evidence of processes that have not been reported before. This study finds evidence of a combined impact of the DE3 and planetary waves on the ionosphere that would be difficult to discern from even multiple ground-based observers.

[30] The results obtained in this study will be useful for numerical simulations of the equatorial ionosphere. Recent studies show that the DE3 is an important driver of longitudinal variability in ionospheric properties [e.g., *Immel et al.*, 2006; *Hagan et al.*, 2007]. Here the study finds strong periodic oscillations, characteristic of planetary waves, in the DE3 signature in the equatorial F region. Models aimed at simulating variations in the equatorial ionosphere should consider the combined effect of tides and planetary waves and possibly the effect of their nonlinear interaction. A comprehensive ionosphere-atmosphere model will provide insights to better understand the underlying processes responsible for the recently observed ionospheric variability.

[31] The meteor radar measurements used in this study also reveal strong 2 day waves during the time period studied here (see Figure 6). The 2 day wave and its impact on the ionosphere have been noted [e.g., *Ito et al.*, 1986; *Chen*, 1992; *Pancheva et al.*, 2006]. It would be interesting to investigate if the 2 day wave observed here produces a corresponding signature in h_mF_2. In the current study, a harmonic fitting for sinusoidal waves has been used to find the periodicity of the wave number 4 structure. Here, the COSMIC data were grouped into n series (n = 4, 5, 6, 7, 8), and the power of the wave number 4 for each of the n series

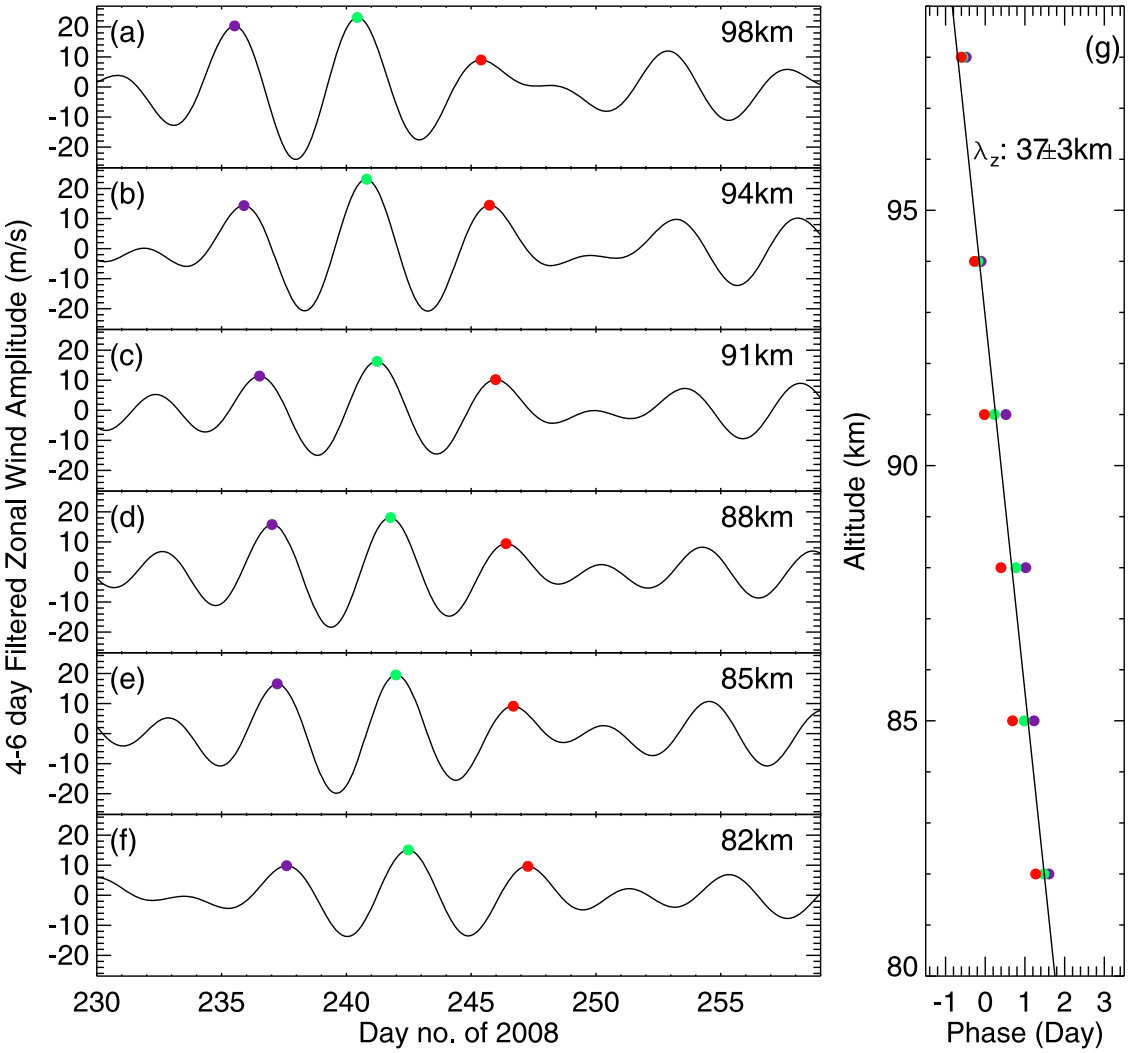

Figure 7. (a)–(f) Amplitude of 4–6 day filtered zonal winds from the SKiYMET radar at Thumba for 82–98 km altitudes over 17 August to 16 September 2008. The colored dots mark the maxima of zonal wind. (g) The phase of the 5 day wave at different altitudes. The straight line is from the linear regression. The slope of this line indicates that the vertical wavelength of the 5 day wave is 37 ± 3 km.

was fitted with a sinusoidal wave with a period of *n* days. This fitting requires more than two data points; thus, this method cannot be used for the 2 day wave. Studying the 2 day wave requires a different method and will be the subject of future work.

[32] **Acknowledgments.** This work is supported by the CEDAR/NSF postdoctoral program. The ISR data are obtained from the MIT Haystack Observatory and the Jicamarca Radio Observatory through the OpenMadrigal. The COSMIC data are obtained from the COSMIC Data Analysis and Archive Center.

[33] Zuyin Pu thanks Dora Pancheva and Gordon Shepherd for their assistance in evaluating this paper.

References

Appleton, E. (1946), Two anomalies in the ionosphere, *Nature*, *157*, 691.

Carruthers, G. R., and T. Page (1976), Apollo 16 far ultraviolet imagery of the polar auroras, tropical airglow belts, and general airglow, *J. Geophys. Res.*, *81*, 483–496.

Chen, P.-R. (1992), Two-day oscillation of the equatorial ionization anomaly, *J. Geophys. Res.*, *97*, 6343–6357.

Cheng, C.-Z., Y.-H. Kuo, R. A. Anthes, and L. Wu (2006), Satellite constellation monitors global and space wether, *Eos Trans. AGU*, *87*, 166–167.

England, S. L., T. J. Immel, E. Sagawa, S. B. Henderson, M. E. Hagan, S. B. Mende, H. U. Frey, C. M. Swenson, and L. J. Paxton (2006), Effect of atmospheric tides on the morphology of the quiet time, postsunset equatorial ionospheric anomaly, *J. Geophys. Res.*, *111*, A10S19, doi:10.1029/2006JA011795.

England, S. L., X. Zhang, T. J. Immel, J. M. Forbes, and R. DeMajistre (2009), The effect of non-migrating tides on the morphology of the equatorial ionospheric anomaly: seasonal variability, *Earth Planets Space*, *61*, 493–503.

Forbes, J. M. (2000), Wave coupling between the lower and upper atmosphere: Case study of an ultra-fast Kelvin Wave, *J. Atmos. Sol. Terr. Phys.*, *62*, 1603–1621.

Forbes, J. M., D. Revelle, and X. Zhang (1996), Longitude structure of the ionosphere *F* region from TOPEX/Poseidon and ground-based data during January 20–30, 1993, including the quasi 2-day oscillation, *J. Geophys. Res*, *102*, 7293–7299.

Forbes, J. M., X. Zhang, S. Palo, J. Russell, C. J. Mertens, and M. Mlynczak (2008), Tidal variability in the ionospheric dynamo region, *J. Geophys. Res.*, *113*, A02310, doi:10.1029/2007JA012737.

Fox, M. W. (1994), A simple, convenient formalism for electron density profiles, *Radio Sci.*, *29*, 1473–1491.

Fritts, D. C., and R. A. Vincent (1987), Mesospheric momentum flux studies at Adelaide, Australia: Observations and a gravity wave-tidal interaction model, *J. Atmos. Sci.*, *44*, 605–619.

Hagan, M. E., and J. M. Forbes (2002), Migrating and nonmigrating diurnal tides in the middle and upper atmosphere excited by tropospheric latent heat release, *J. Geophys. Res.*, *107*(D24), 4754, doi:10.1029/2001JD001236.

Hagan, M. E., and J. M. Forbes (2003), Migrating and nonmigrating semidiurnal tides in the upper atmosphere excited by tropospheric latent heat release, *J. Geophys. Res.*, *108*(A2), 1062, doi:10.1029/2002JA009466.

Hagan, M. E., A. Maute, R. G. Roble, A. D. Richmond, T. J. Immel, and S. L. England (2007), Connections between deep tropical clouds and the Earth's ionosphere, *Geophys. Res. Lett.*, *34*, L20109, doi:10.1029/2007GL030142.

Hagan, M. E., A. Maute, and R. G. Roble (2009), Tropospheric tidal effects on the middle and upper atmosphere, *J. Geophys. Res.*, *114*, A01302, doi:10.1029/2008JA013637.

Hartman, W. A., and R. A. Heelis (2007), Longitudinal variations in the equatorial vertical drift in the topside ionosphere, *J. Geophys. Res.*, *112*, A03305, doi:10.1029/2006JA011773.

Heelis, R. A., W. R. Coley, A. G. Burrell, M. R. Hairston, G. D. Earle, M. D. Perdue, R. A. Power, L. L. Harmon, B. J. Holt, and C. R. Lippincott (2009), Behavior of the O^+/H^+ transition height during the extreme solar minimum of 2008, *Geophys. Res. Lett.*, *36*, L00C03, doi:10.1029/2009GL038652.

Henderson, S. B., C. M. Swenson, A. B. Christensen, and L. J. Paxton (2005), Morphology of the equatorial anomaly and equatorial plasma bubbles using image subspace analysis of Global Ultraviolet Imager data, *J. Geophys. Res.*, *110*, A11306, doi:10.1029/2005JA011080.

Hirota, I. (1979), Kelvin waves in the equatorial middle atmosphere observed by the Nimbus 5 SCR, *J. Atmos. Sci.*, *36*, 217–222.

Immel, T. J., E. Sagawa, S. L. England, S. B. Henderson, M. E. Hagan, S. B. Mende, H. U. Frey, C. M. Swenson, and L. J. Paxton (2006), Control of equatorial ionospheric morphology by atmospheric tides, *Geophys. Res. Lett.*, *33*, L15108, doi:10.1029/2006GL026161.

Immel, T. J., S. L. England, X. Zhang, J. M. Forbes, and R. DeMajistre (2009), Upward propagating tidal effects across the E- and F-regions of the ionosphere, *Earth Planets Space*, *61*, 1–11.

Ito, R., S. Kato, and T. Tsuda (1986), Consideration of an ionospheric dynamo driven by a planetary wave with a two-day period, *J. Atmos. Terr. Phys.*, *48*, 1–13.

Kelley, M. C., V. K. Wong, N. Aponte, C. Coker, A. J. Mannucci, and A. Komjathy (2009), Comparison of COSMIC occultation-based electron density profiles and TIP observations with Arecibo incoherent scatter radar data, *Radio Sci.*, *44*, RS4011, doi:10.1029/2008RS004087.

Kumar, K. K., G. Rankumar, and S. T. Shelbi (2007), Initial results from SKiYMET meteor radar at Thumba (8.5°N, 77°E): 1. Comparison of wind measurements with MF spaced antenna radar system, *Radio Sci.*, *42*, RS6008, doi:10.1029/2006RS003551.

Kumar, K. K., V. Deepa, M. Antonita, and G. Ramkumar (2008), Meteor radar observations of short-term tidal variabilities in the low-latitude mesosphere-lower thermosphere: Evidence for nonlinear wave-wave interactions, *J. Geophys. Res.*, *113*, D16108, doi:10.1029/2007JD009610.

Laštovička (2006), Forcing of the ionosphere by waves from below, *J. Atmos. Sol. Terr. Phys.*, *68*, 479–497.

Lei, J., et al. (2007), Comparison of COSMIC ionospheric measurements with ground-based observations and model predictions: Preliminary results, *J. Geophys. Res.*, *112*, A07308, doi:10.1029/2006JA012240.

Lin, C. H., W. Wang, M. E. Hagan, C. C. Hsiao, T. J. Immel, M. L. Hsu, J. Y. Liu, L. J. Paxton, T. W. Fang, and C. H. Liu (2007), Plausible effect of atmospheric tides on the equatorial ionosphere observed by the FORMOSAT3/COSMIC: Three-dimensional electron density structure, *Geophys. Res. Lett.*, *34*, L11112, doi:10.1029/2007GL029265.

Mukhtarov, P., D. Pancheva, and B. Andonov (2009), Global structure and interannual variability of the migrating diurnal tide seen in the SABER/TIMED temperatures between 20 and 120 km, *J. Geophys. Res.*, *114*, A02309, doi:10.1029/2008JA013759.

Namba, S., and K. I. Maeda (1939), *Radio Wave Propagation*, Corona, Tokyo.

Oberheide, J., and J. M. Forbes (2008), Tidal propagation of deep tropical cloud signatures into the thermosphere from TIMED observations, *Geophys. Res. Lett.*, *35*, L04816, doi:10.1029/2007GL032397.

Pancheva, D. V., et al. (2006), Two-day wave coupling of the low-latitude atmosphere-ionosphere system, *J. Geophys. Res.*, *111*, A07313, doi:10.1029/2005JA011562.

Pancheva, D. V., et al. (2008), Planetary wave coupling (5–6 day waves) in the low-latitude atmosphere-ionosphere system, *J. Atmos. Sol. Terr. Phys.*, *70*, 101–122.

Pancheva, D. V., P. Mukhtarov, B. Andonov, N. J. Mitchell, and J. M. Forbes (2009a), Planetary waves observed by TIMED/SABER in coupling the stratosphere-mesosphere- lower thermosphere during the winter of 2003/2004: 1. Comparison with the UKMO temperature results, *J. Atmos. Sol. Terr. Phys.*, *71*, 61–74.

Pancheva, D. V., P. Mukhtarov, B. Andonov, N. J. Mitchell, and J. M. Forbes (2009b), Planetary waves observed by TIMED/SABER in coupling the stratosphere-mesosphere- lower thermosphere during the winer of 2003/2004: 2. Altitude and latitude planetary wave structure, *J. Atmos. Sol. Terr. Phys.*, *71*, 75–87.

Pedatella, N. M., and J. M. Forbes (2009), Modulation of the equatorial F-region by the quasi-16-day planetary wave, *Geophys. Res. Lett.*, *36*, L09105, doi:10.1029/2009GL037809.

Sagawa, E., T. J. Immel, H. U. Frey, and S. B. Mende (2005), Longitudinal structure of the equatorial anomaly in the nighttime ionosphere observed by IMAGE/FUV, *J. Geophys. Res.*, *110*, A11302, doi:10.1029/2004JA010848.

Scherliess, L., D. C. Thompson, and R. W. Schunk (2008), Longitudinal variability of low-latitude total electron content: Tidal influences, *J. Geophys. Res.*, *113*, A01311, doi:10.1029/2007JA012480.

Schreiner, W., C. Rochen, S. Sokolovskiy, S. Syndergaard, and D. Hunt (2007), Estimates of the precision of GPS radio occultations from the COSMIC/FORMOSAT-3 mission, *Geophys. Res. Lett.*, *34*, L04808, doi:10.1029/2006GL027557.

Schunk, R. W., and A. F. Nagy (2000), *Ionospheres Physics, Plasma Physics, and Chemistry*, Cambridge Univ. Press, Cambridge, U. K.

Takahashi, H., et al. (2006), Signatures of 3–6 day planetary waves in the equatorial mesosphere and ionosphere, *Ann. Geophys.*, *24*, 3343–3350.

Teitelbaum, H., and F. Vial (1991), On tidal variability induced by nonlinear interaction with planetary waves, *J. Geophys. Res.*, *96*, 14,169–14,178.

Thuillier, G., R. H. Wiens, G. G. Shepherd, and R. G. Roble (2002), Photochemistry and dynamics in thermospheric intertropical arcs measured by the WIND Imaging Interferometer on board UARS: A comparison with TIE-GCM simulations, *J. Atmos. Sol. Terr. Phys.*, *64*, 405–415.

Wu, D. L., P. B. Hays, and W. R. Skinner (1994), Observations of the 5-day wave in the mesosphere and lower thermosphere, *Geophys. Res. Lett.*, *21*, 2733–2736.

S. L. England, T. J. Immel, and G. Liu, Space Sciences Laboratory, University of California, Berkeley, CA 94720, USA. (guiping@ssl.berkeley.edu)

K. K. Kumar and G. Ramkumar, Space Physics Laboratory, Vikram Sarabhai Space Centre, Trivandrum 695022, India.